Contents lists available at ScienceDirect

# Biochemical and Biophysical Research Communications

# A novel approach to the identification and quantitative elemental analysis of amyloid deposits—Insights into the pathology of Alzheimer's disease

Reshmi Rajendran [a], Ren Minqin [a], Maria Dolores Ynsa [b], Gemma Casadesus [c], Mark A. Smith [d], George Perry [d], Barry Halliwell [e], Frank Watt [a,*]

[a] Centre for Ion Beam Applications, Department of Physics, Blk S 12, Faculty of Science, National University of Singapore, 2, Science Drive 3, Singapore 117542, Singapore
[b] Centro de Micro-Analisis de Materiales (CMAM), Universidad Autonoma de Madrid, Campus de Cantoblanco, 28049 Madrid, Spain
[c] Department of Neurosciences, Case Western Reserve University, Cleveland, OH 44106, USA
[d] Department of Pathology, Case Western Reserve University, Cleveland, OH 44106, USA
[e] Department of Biochemistry, National University of Singapore, Singapore

## ARTICLE INFO

## ABSTRACT

There is considerable interest in the role of metals such as iron, copper, and zinc in amyloid plaque formation in Alzheimer's disease. However to convincingly establish their presence in plaques in vivo, a sensitive technique is required that is both quantitatively accurate and avoids isolation of plaques or staining/fixing brain tissue, since these processes introduce contaminants and redistribute elements within the tissue. Combining the three ion beam techniques of scanning transmission ion microscopy, Rutherford back scattering spectrometry and particle induced X-ray emission in conjunction with a high energy (MeV) proton microprobe we have imaged plaques in freeze-dried *unstained* brain sections from CRND-8 mice, and simultaneously quantified iron, copper, and zinc. Our results show increased metal concentrations within the amyloid plaques compared with the surrounding tissue: iron (85 ppm compared with 42 ppm), copper (16 ppm compared to 6 ppm), and zinc (87 ppm compared to 34 ppm).

© 2009 Elsevier Inc. All rights reserved.

## Introduction

Alzheimer's disease (AD) is characterized, among other things, by the presence of $\beta$ amyloid (A$\beta$) deposits in the brain, the accumulation of which is considered an early and important event in AD development [1]. Various factors have been implicated in the etiology of the disease; oxidative stress being among one of the widely accepted ones [2]. The oxidative stress theory is supported by the widespread lipid peroxidation, protein oxidation, and DNA oxidation seen in AD brains [3,4]. In addition, pro-oxidants increase A$\beta$ production [5,6] and several antioxidants, namely vitamin E and melatonin, can protect isolated neurons from A$\beta$-induced toxicity [7–11] further reinforcing the theory.

Even though the most damaging effects of oxidative damage and the corresponding antioxidant responses in AD are well characterized, the sources of damaging reactive oxygen species (ROS) are yet to be established [12]. The brain has a relatively high concentration of biometals (iron, copper, and zinc) [13], so a metal-centered mechanism might be at work, e.g., converting hydrogen peroxide (H$_2$O$_2$) to the highly reactive hydroxyl radical (OH$^.$). Many recent studies implicate biometals in the development or progression of Alzheimer's disease [14–22].

Of these biometals, iron and copper are significant because of their ability to catalyze oxidative damage [23]. They have also been shown to induce aggregation of A$\beta$ under normal [24] and under mildly acidic conditions (similar to the AD brain) without fibril formation [25]. Moreover, human A$\beta$ directly produces H$_2$O$_2$ by a mechanism that involves metal ions, Fe (III) or Cu (II), setting up conditions for Fenton-type chemistry [26]. Elevated copper has also been held responsible for causing the covalent cross-linking of A$\beta$ in senile plaques [27]. Zinc is relevant because of its supposed ability to modulate APP processing [28] leading to a greater deposition of A$\beta$ and its ability to bind A$\beta$ in vitro [29], leading to increased aggregation.

In order to elucidate the role of these metals, which occur in trace amounts in tissue, a technique is required which can identify amyloid deposits (one of the major characteristics of AD) and simultaneously quantify these trace elements within them *without recourse to conventional fixing and staining*, since these processes are known to cause trace element redistribution and contamination. Contamination has been a major problem in previous studies, e.g., early studies indicating that aluminum was associated with amyloid deposition were shown to be an artifact of the staining

---

* Corresponding author. Fax: +65 6777 6126.
  E-mail address: phywattf@nus.edu.sg (F. Watt).

process [30]. Plaque isolation methods are also unreliable since this involves homogenization of brain tissue, which can liberate metal ions [31] that could then bind to plaques. Microprobe techniques are most suitable for assessing morphological and elemental alteration in tissue. Although studies carried out using various microprobe techniques have indicated an increase of iron, copper, and zinc in Alzheimer's disease, they have all been carried out on *stained* tissue, which carries a high risk of amyloid contamination.

Here, we describe a novel technique which can be used to identify plaques in Alzheimer's transgenic mice and simultaneously map and quantify the elemental distribution within them. Nuclear microscopy is a suite of imaging techniques composed of scanning transmission ion microscopy (STIM), Particle induced X-ray emission (PIXE) and Rutherford back scattering (RBS) used in conjunction with a MeV proton microprobe [32]. Using STIM for structural identification, RBS for matrix characterization, and PIXE for trace elemental analysis, we are able to image and identify amyloid plaques in brain sections from transgenic mice and simultaneously map and quantify the trace elements within them. Random areas devoid of plaques in the transgenic mice brain and in the age-matched control sample were also examined for comparative quantitative analysis.

## Materials and methods

*Sample preparation.* The tissue was harvested from Alzheimer's transgenic CRND-8 mouse brain. CRND-8 encodes a double mutant form of amyloid precursor protein 695 (KM670/671NL + V717F) under the control of the PrP gene promoter [33]. These animals show Thioflavin S-positive Aβ deposits at 3 months, with dense-cored plaques and neuritic pathology evident from 5 months of age. Nuclear microscopy experiments were carried out on five test mice, 6 months old, with confirmed AD pathology in various brain regions compared to the age-matched control. Cryofixation, where tissue and cells are rapidly frozen to preserve their elemental integrity is considered to be the best way of preparing samples for trace element studies [34,35]. The animals were perfused with saline. Brains were extracted, cut sagittally through the mid-section, immersed in isopentane, and immediately frozen with liquid nitrogen. The samples were transported on dry ice when required (thereby maintaining subzero temperatures to prevent thawing and minimizing subsequent ice crystal damage) and stored at −80 °C. The sections were cut using a Leica CM3050S cryostat, with the temperature set at −17 °C and the object holder at −22 °C. Twenty micrometers was found to be a suitable thickness for both nuclear microscopy analysis and staining. Sections for nuclear microscopy analysis picked up on freshly made thin organic pioloform films about 0.5 μm thick were stored in a freezer at −20 °C. Adjacent sections which were picked up on gelatin coated slides were immediately processed.

*Immunohistochemical staining (to confirm the distribution of amyloid).* For Aβ immunohistochemistry, the sections were stained free floating. The sections were immunostained with a 1:5000 dilution of primary amyloid-β antibody (0.164 mg/ml) (mouse monoclonal; Biosource), a goat anti-mouse secondary antibody and an avidin–biotin–HRP complex (details in Vectastatin Elite ABC kit, Vector, Burlingame, CA). Incubation times were 24 h (at 4 °C) for the primary antibody, 30 min (at room temperature) for the secondary antibody, and 1 h (at room temperature) for the avidin–biotin–HRP complex. Sections were treated with DAB, rinsed, and mounted on superfrost and gelatinized slides.

*Nuclear microscopy analysis.* The nuclear microscopy experiments were carried out at the Centre for Ion Beam Applications, CIBA, at the National University of Singapore. A 2.1 MeV proton beam focused to a 1 μm spot size was used. Data from the three

techniques of particle induced X-ray emission (PIXE) for trace elemental analysis, Rutherford backscattering spectrometry (RBS) to measure the concentration of matrix constituents of the sample and scanning transmission ion microscopy (STIM) to identify regions of interest in the specimen, were simultaneously collected.

Scanning transmission ion microscopy (STIM) is a technique used to investigate samples which are thin enough for transmission of a 2–3 MeV proton beam. For relatively thin organic samples (30 μm or less), essentially all incident protons that have not suffered nuclear backscattering will pass through the sample. Measurement of the energy or the energy loss of the transmitted proton gives information on the density structure of the sample. Particle induced X-ray emission (PIXE) is a well-established technique for trace elemental analysis offering non-destructive multi-elemental capability and low detection limits. It allows simultaneous detection of several elements, with a sensitivity of about 1 ppm in biological material such as tissue sections and cells [36].

The X-ray and RBS energy spectra were obtained from regions of interest (ROI) after careful identification of amyloid deposits from the STIM maps. The data obtained from RBS allowed quantification of light matrix elements such as C, N, and O. Fitting the RBS spectra using SIMNRA [37] software in conjunction with Dan32 software allowed us to measure the areal density. This technique was also used for integrated charge correction, thus enabling quantitative data pertaining to the elemental concentrations down to the parts per million of the ROI to be extracted from the PIXE spectra by Dan32 [38]. Statistical comparison was carried out between the different ROI using means and standard errors (as the sample size was finite). Significant differences for the elemental concentrations between and among groups were determined using the parametric Student's *t*-test [39]. Differences were considered significant when a confidence interval of 95% was exceeded ($P < 0.05$).

## Results

### STIM mapping and plaque identification

Scanning transmission ion microscopy (STIM) was utilized to identify amyloid deposits in tissue without staining. The brains from transgenic mice were cut sagittally through the mid-section, and serial sections (20 μm) were taken. For each section mounted on a target holder for nuclear microscopy, an adjacent section was picked up on a gelatin coated slide for amyloid staining using immunohistochemical methods. The area of interest was identified on the basis of structural landmarks in the tissue. The β-pleated structure of the Aβ protein, of which the plaque cores are composed, is denser than the surrounding tissue—from our calculations we observed a 12% increase in the dry density of the plaque compared to the background tissue and the control samples. Thus, plaques can be rapidly identified in unstained tissue by imaging tissue density distributions using STIM. Similar numbers of plaques per unit area were observed in both the stained sections, and in the untreated sections analyzed using STIM (Fig. 1).

### PIXE analysis

PIXE is a non-destructive technique that allows simultaneous multi-trace elemental analysis down to the parts per million levels. The elemental concentration of 10 plaques from each of the five test samples and three areas devoid of plaques from the background tissue of each sample and from the non-transgenic control were measured. An elemental comparison between the amyloid plaque and the surrounding tissue revealed an increase of phosphorus, sulfur, potassium, calcium, iron, copper, and zinc in the
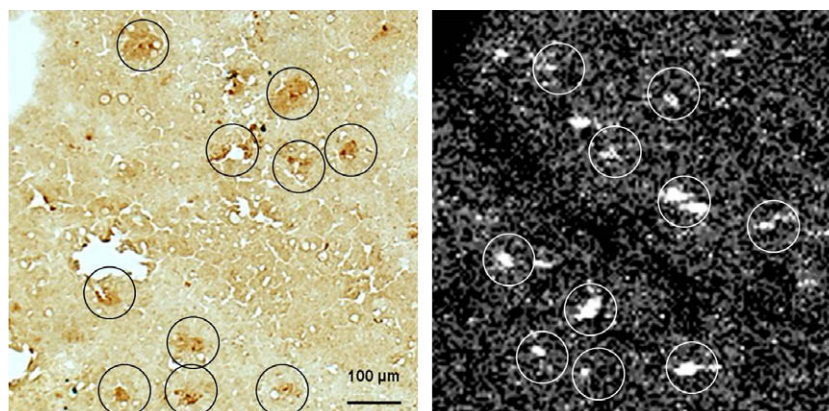
**Fig. 1.** Correlation between a tissue section where the amyloid deposits are identified using immunohistochemical staining (lhs) and the STIM image from the same region from an *unstained* serial section (rhs).

plaque compared to the average concentration of the background tissue and control (Table 1). Interestingly, the unaffected parts of the transgenic mice exhibited similar elemental concentrations to a control brain (Table 1). The trace element concentrations were consistently elevated in all plaques examined. A significant increase in Fe, Zn, and Cu was observed in the plaques compared to the background ($P < 0.05$) and a significant increase in Zn and Fe ($P < 0.05$) compared with the non-transgenic control (Fig. 2). Unlike other microscopic techniques, where comparison is based on the number of detected events per unit volume/area, our technique enables us to normalize to the density of the tissue, thus ensuring that the increase in elements observed is not an artifact due to an increase in local density or changes in tissue section thickness. A comparison based only on the proton induced X-ray

**Table 1**
The average elemental concentrations (parts per million–dry weight) in the amyloid plaques compared to the background tissue from the transgenic mice and the age-matched control.

|   | Plaque | | Background (test) | | Control | |
|---|---|---|---|---|---|---|
|   | PPM | SE | PPM | SE | PPM | SE |
| P | 15889.0 | 992.6 | 9068.2 | 821.2 | 9493.0 | 499.9 |
| S | 7261.6 | 536.0 | 4533.4 | 424.3 | 4962.6 | 364.2 |
| K | 21636.1 | 2041.5 | 11884.6 | 1192.0 | 11180.8 | 760.9 |
| Ca | 304.1 | 58.5 | 196.9 | 22.6 | 159.6 | 15.5 |
| Fe | **85.3** | 14.6 | **42.7** | 9.2 | **41.3** | 0.2 |
| Cu | **16.4** | 3.5 | **5.9** | 1.8 | **6.4** | 4.5 |
| Zn | **86.9** | 16.2 | **34.1** | 12.1 | **20.1** | 6.4 |



**Fig. 2.** Iron, copper, and zinc concentrations (parts per million–dry weight) of the analyzed amyloid plaques compared to the background tissue from the transgenic mice and the age-matched control.

counts without density normalization also indicates an increase in all the elements, including iron, copper, and zinc in the plaques compared to the background (Fig. 3). This explains why, in other studies, an increase of most elements is seen. By themselves, the results from these studies cannot be considered absolute, as the increase observed could be an artifact due to an increase in density.

## Discussion

We have shown that a combination of the three techniques of STIM, RBS, and PIXE can identify plaques in unstained tissue from brain slices and quantify the elements within them. Neuritic plaques in human brain tissue, which have a characteristic shape, have been previously identified using off-axis STIM [30]. However, since the focus of that work was to optimize the conditions for the identification of aluminum, simultaneous trace elemental analysis of the transition metals was not carried out. We calculated that the amyloid deposits are denser than background tissue; a 12% increase in the dry density of the plaque compared to the background tissue and the control samples, was observed, thus enabling rapid identification by STIM.
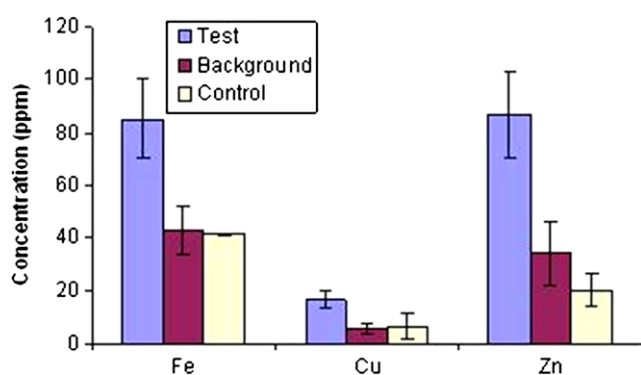
We are the first group to have carried out μ-PIXE trace element analysis on amyloid plaques in *unstained* tissue. The trace elemental analysis revealed a significant increase of most metals, including iron (85 ppm compared with 42 ppm), copper (16 ppm compared to 6 ppm), and zinc (87 ppm compared to 34 ppm) in the amyloid deposits when compared to the surrounding tissue and to the controls. Our work supports the theory that redox interactions between Aβ and metals could be at the heart of a pathological feedback system wherein Aβ amyloidosis and oxidative stress promote each other, possibly via Fenton chemistry [40,41].

Previous studies on amyloid plaques have always been carried out on *stained* tissue. Examples are Synchrotron FTIRM and Synchrotron SXRF studies on Thioflavin S-positive stained amyloid deposits [42], LA-ICP-MS studies on plaques labeled with Eu- and Ni-coupled antibodies [43] and micro PIXE studies on amyloid plaques visualized using two staining methods; an anti-Tau 2 antibody and an antibody to Aβ (10D-5) [44]. Using synchrotron X-rays, increased iron compounds were detected in the superior frontal gyrus of Alzheimer's disease patients in *unstained* tissue and fluorescently mapped using XANES and XFS [45], but it was beyond the scope of these techniques to correlate the increased iron with any of the characteristic pathology of AD.
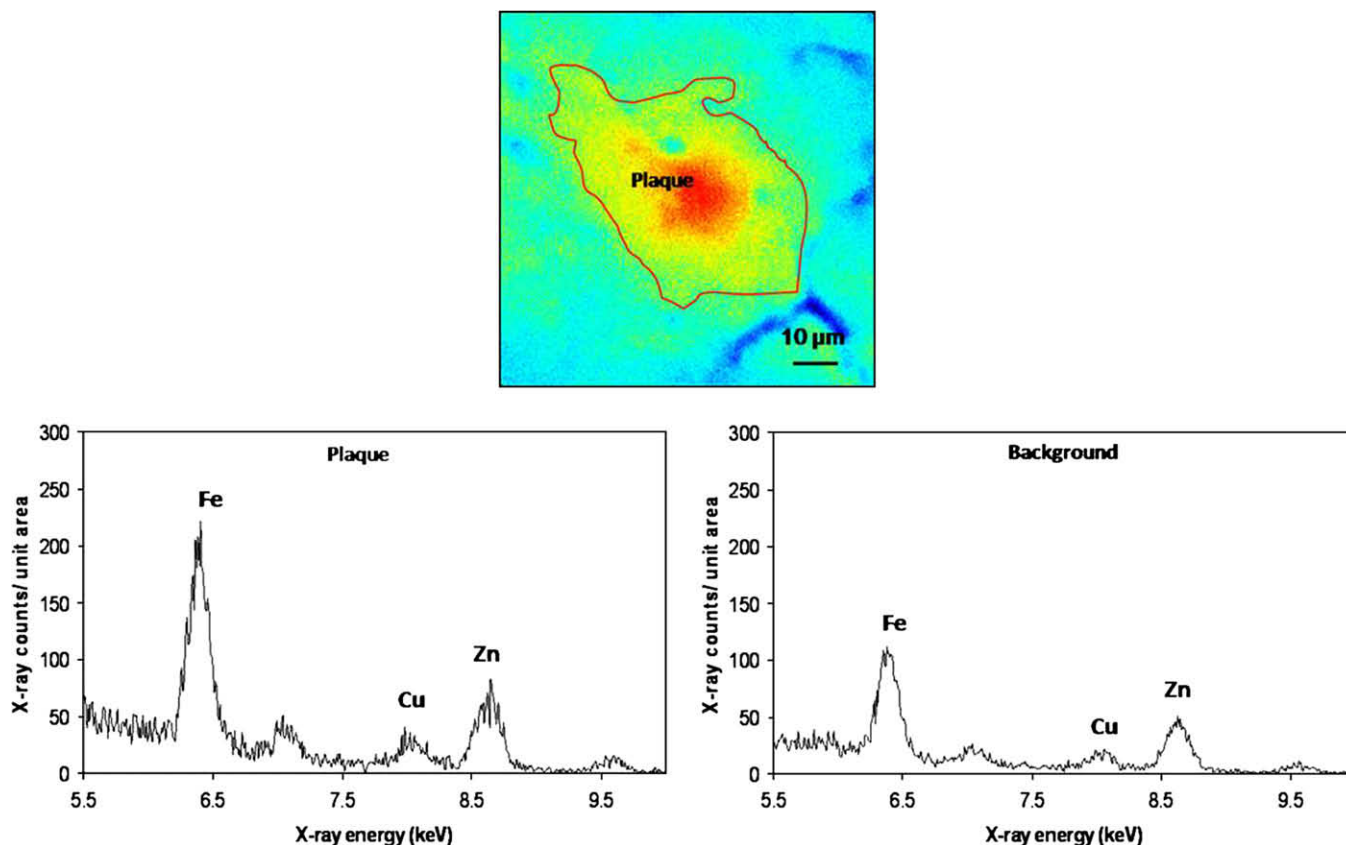
Our technique, carried out on unstained tissue and normalized to density gives us definite results of the elemental status of the plaques compared to the background and the control. As transgenic mice were used for the study, a further time sequence study

**Fig. 3.** STIM image of an amyloid plaque (top) and X-ray counts/unit area from the PIXE spectra for iron, copper, and zinc in the amyloid plaque (calculated from within the area denoted by the red outline in the STIM map above) compared to the background (the rest of the area). (For interpretation of the references to color in this figure legend, the reader is referred to the web version of this paper.)

of the development and quantitative trace elemental concentration variation with development of the deposits is now possible.

## References

[1] D.J. Selkoe, Biochemistry and molecular biology of amyloid beta-protein and the mechanism of Alzheimer's disease, Handb. Clin. Neurol. 89 (2008) 245–260.
[2] D.A. Butterfield, T. Reed, F. Shelley, F. Newman, R. Sultana, Role of amyloid β-peptide-associated oxidative stress and brain protein modifications in the pathogenesis of Alzheimer's disease and mild cognitive impairment, Free Radic. Biol. Med. 43 (2007) 658–677.
[3] B. Halliwell, Role of free radicals in the neurodegenerative diseases: therapeutic implications for antioxidant treatment, Drugs Aging 18 (9) (2001) 685–716.
[4] B. Halliwell, Oxidative stress and neurodegeneration: where are we now?, J Neurochem. 97 (6) (2006) 1634–1658.
[5] D.C. Paola, M. Nitti, A. Vitali, R. Borghi, D. Cottalasso, D. Zaccheo, P. Odetti, P. Strocchi, U.M. Marinari, M. Tabaton, M.A. Pronzato , Oxidative stress induces increase in intracellular amyloid β-protein production and selective activation of βI and βII PKCs in NT2 cells, Biochem. Biophys. Res. Commun. 268 (2000) 642–646.
[6] E. Tamagno, M. Parola, P. Bardini, A. Piccini, R. Borghi, M. Guglielmotto, G. Santoro, A. Davit, O. Danni, M.A. Smith, G. Perry, M. Tabaton, Beta-site APP cleaving enzyme up-regulation induced by 4-hydroxynonenal is mediated by stress-activated protein kinases pathways, J. Neurochem. 92 (2005) 628–636.
[7] R. Resende, P.A. Moreira, T. Proeca, A. Deshpande, J. Busciglio, C. Pereira, C.R. Oliveira, Brain oxidative stress in a triple-transgenic mouse model of Alzheimer's disease, Free Radic. Biol. Med. 44 (2008) 2051–2057.
[8] S.M. Cardoso, C.R. Oliveira, Glutathione cycle impairment mediates A beta induced cell toxicity, Free Radic. Res. 37 (2003) 241–250.
[9] J.B. Melo, P. Agostinho, C.R. Oliveira, Involvement of oxidative stress in the enhancement of acetylcholinesterase activity induced by amyloid beta-peptide, Neurosci. Res. 45 (2003) 117–127.
[10] R.G. Cutler, J. Kelly, K. Storie, W.A. Pedersen, A. Tammara, K. Hatanpaa, J.C. Troncoso, M.P. Mattson, Involvement of oxidative stress-induced abnormalities in ceramide and cholesterol metabolism in brain aging and Alzheimer's disease, Proc. Natl. Acad. Sci. USA 101 (2004) 2070–2075.
[11] J.H. Jhoo, H.C. Kim, T. Nabeshima, K. Yamada, E.J. Shin, W.K. Jhoo, W. Kim, K.S. Kang, S.A. Jo, J.I. Woo, Beta-amyloid (1–42)-induced learning and memory deficits in mice. Involvement of oxidative burdens in the hippocampus and cerebral cortex, Behav. Brain Res. 155 (2004) 185–196.
[12] L.M. Sayre, G. Perry, P.L.R. Harris, Y. Liu, K.A. Schubert, M.A. Smith, Oxidative damage to mitochondrial DNA is increased in Alzheimer's disease, J. Neurochem. 74 (1) (2000) 270.
[13] A.I. Finkelstein, T. Lynch, S. Wilkins, R.A. Cherny, A.I. Bush, Metals, Oxidative Stress and Brain Biology. Encyclopedia of Stress, Elsevier Science, Oxford, 2007.
[14] S. Bolognin, P. Zatta, D. Drago, P.P. Parnigotto, F. Richelli, G. Tognon, Mutual stimulation of beta-amyloid fibrillogenesis by clioquinol and divalent metals, Neuromol. Med. 10 (4) (2008) 322–332.
[15] A.I. Bush, The metallobiology of Alzheimer's disease, Trends Neurosci. 26 (4) (2003) 207–214.
[16] M.P. Cuajunco, C.J. Frederickson, A.I. Bush, Amyloid-beta metal interaction and metal chelation, Subcell. Biochem. 38 (2005) 235–254.
[17] J. Ryu, K. Girigoswami, K. Ha, S.H. Ku, C.B. Park, Influence of multiple metal ions on beta-amyloid aggregation and dissociation on a solid surface, Biochemistry 47 (19) (2008) 5328–5335.
[18] I. Shcherbatykh, D.O. Carpenter, The role of metals in the etiology of Alzheimer's disease, J. Alzheimers Dis. 11 (2) (2007) 191–205.
[19] D.G. Smith, R. Cappai, K.J. Barnham, The redox chemistry of the Alzheimer's disease amyloid beta peptide, Biochim. Biophys. Acta 1768 (8) (2007) 1976–1990.
[20] P.A. Adlard, A.I. Bush, Metals and Alzheimer's disease, J. Alzheimers Dis. 10 (2-3) (2006) 145–163.
[21] R.R. Crichton, D.T. Dexter, J.W. Roberta, Metal based neurodegenerative diseases—from molecular mechanisms to therapeutic strategies, Coord. Chem. Rev. 251 (10–11) (2008) 1189–1199.
[22] K.J. Barnham, A.I. Bush, Metals in Alzheimer's and Parkinson's diseases, Curr. Opin. Chem. Biol. 12 (2) (2008) 222–228.
[23] B. Halliwell, J.M.C. Gutteridge, Free Radicals in Biology and Medicine, fourth ed., Oxford University Press, Oxford, 2007.

[24] X. Huang, C.S. Atwood, R.D. Moir, M.A. Hartshorn, R.E. Tanzi, A.I. Bush, Trace metal contamination initiates the apparent and oligomerization of Alzheimer's Abeta peptides auto-aggregation amyloidosis, J. Biol. Inorg. Chem. 9 (8) (2004) 954–960.

[25] A.I. Bush, R.D. Moir, K.M. Rosenkranz, R.E. Tanzi, Response, Science 268 (5219) (1995) 1921–1923.

[26] A.I. Bush, The metallobiology of Alzheimer's disease, Trends Neurosci. 26 (4) (2003) 207–214.

[27] C.S. Atwood, G. Perry, H. Zeng, Y. Kato, W.D. Jones, K.Q. Ling, X. Huang, R.D. Moir, D. Wang, L.M. Sayre, M.A. Smith, S.G. Chen, A.I. Bush, Copper mediates dityrosine cross-linking of Alzheimer's amyloid-beta, Biochemistry 43 (2) (2004) 560–568.

[28] C.J. Maynard, A.I. Bush, C.L. Masters, R. Cappai, Q.X. Li, Metals and amyloid-β in Alzheimer's disease, Int. J. Exp. Pathol. 86 (2005) 147.

[29] A.I. Bush, W.H. Pettingell, M.D. Paradis, R.E. Tanzi, W. Wasco, The amyloid β-protein precursor and its mammalian homologues, J. Biol. Chem. 269 (43) (1994) 26618–26621.

[30] J.P. Landsberg, B. McDonald, F. Watt, Absence of aluminium in neuritic plaque cores in Alzheimer's disease, Nature 360 (1992) 65–67.

[31] J.P.E. Spencer, A. Jenner, O.I. Aruoma, P.J. Evans, H. Kaur, D.T. Dexter, P. Jenner, A.J. Lees, D.C. Marsden, B. Halliwell, Intense oxidative DNA damage promoted by L-DOPA and its metabolites—implications for neurodegenerative disease, FEBS Lett. 353 (1994) 246–250.

[32] F. Watt, J. van Kan, I. Rajta, A.A. Bettiol, T.F. Choo, M.B.H. Breese, T. Osipowicz, The NUS high energy ion nanoprobe facility, Nucl. Instr. Methods 210 (2003) 14–20.

[33] M.A. Chishti, D.-S. Yang, C. Janus, A.L. Phinney, P. Horne, J. Pearson, R. Strome, N. Zuker, J. Loukides, J. French, S. Turner, G. Lozza, M. Grilli, S. Kunicki, C. Morissette, J. Paquette, F. Gervais, C. Bergeron, P.E. Fraser, G.A. Carlson, P.St. George-Hyslop, D. Westaway, Early onset amyloid-deposition and cognitive defects in transgenic mice expressing a double mutant form of amyloid precursor protein 695, J. Biol. Chem. 276 (24) (2001) 21562–21570.

[34] N. Roos, A.J. Morgan, Cryopreparation of Thin Biological Specimens for Electron Microscopy: Methods and Applications, Microscopy Handbooks No. 21, Oxford Science Publications, Oxford, 1990.

[35] A.W. Robards, U.B. Sleytr, Low Temperature Methods in Biological Electron Microscopy—Practical Methods in Electron Microscopy, Elsevier, Amsterdam, 1985. vol. 10.

[36] S.A.E. Johansson, J.L. Campbell, K.G. Malmqvist, Particle Induced X-Ray Emission Spectrometry (PIXE), John Wiley & Sons, Great Britain, 1995.

[37] Mayer Simnra Users' Guide, Technical Report PP 9/113, Max-Planck Institut for Plasmaphysik, Garching, Germany, 1997.

[38] J.A. Maxwell, J.L. Campbell, W.J. Tesdale, The Guelph PIXE software package, Nucl. Instr. Methods B 43 (1989) 218.

[39] R.F. Woolson, Statistical Methods for the Analysis of Biomedical Data, John Wiley & Sons, New York, 1987.

[40] X. Hunag, R.D. Mori, R.E. Tanzi, A.I. Bush, J.T. Rogers, Redox models oxidative stress and Alzheimer's disease pathology, Ann. NY Acad. Sci. 1012 (2004) 153–163.

[41] P. Hajieva, C. Behl, Antioxidants as a potential therapy against age related neurodegenerative diseases: amyloid Beta toxicity and Alzheimer's disease, Curr. Pharm. Des. 12 (6) (2006) 699–704.

[42] L.M. Miller, Q. Wang, T.P. Telivala, R.J. Smith, A. Lanzirotti, J. Miklossy, Synchroton-based infrared and X-ray imaging shows focalized accumulation of Cu and Zn co-localised with β-amyloid deposits in Alzheimer's disease, J. Struct. Biol. 155 (2006) 30–37.

[43] R.W. Hutchinson, A.G. Cox, C.W. McLeod, P.S. Marshall, A. Harper, E.L. Dawson, D.R. Howlett, Imaging and spatial distribution of β-amyloid peptide and metal ions in Alzheimer's plaques by laser ablation-inductively coupled plasma-mass spectrometry, Anal. Biochem. 346 (2) (2005) 225–233.

[44] M.A. Lovell, J.D. Robertson, W.J. Teesdale, J.L. Campbell, W.R. Marksbery, Copper, iron and zinc in Alzheimer's disease senile plaques, J. Neurol. Sci. 158 (1993) 47–52.

[45] J.F. Collingwood, A. Milkhaylova, M.R. Davidson, C. Batich, W.J. Streit, T.E. Skin, J. Terry, R. Barrea, R.S. Underhill, J. Dobson, J. Phys.: Conf. Ser. 17 (2005) 54–60.